Hindawi
Journal of Nanomaterials
Volume 2021, Article ID 5527519, 17 pages
https://doi.org/10.1155/2021/5527519

Research Article

Novel Eco-Friendly Synthesis of Biosilver Nanoparticles as a Colorimetric Probe for Highly Selective Detection of Fe (III) Ions in Aqueous Solution

Nguyen Le Nhat Trang,[1] **Van-Tuan Hoang**,[1] **Ngo Xuan Dinh**,[1] **Le Thi Tam**,[2] **Van Phan Le**,[3] **Dong Thi Linh**,[4] **Doan Manh Cuong**,[5] **Nguyen Tien Khi**,[1] **Nguyen Ha Anh**,[1] **Pham Tuyet Nhung**,[1] **and Anh-Tuan Le**[1,6]

[1]*Phenikaa University Nano Institute (PHENA), Phenikaa University, Hanoi 12116, Vietnam*
[2]*Advanced Institute for Science and Technology (AIST), Hanoi University of Science and Technology (HUST), 01 Dai Co Viet Street, Hai Ba Trung, Ha Noi 10000, Vietnam*
[3]*College of Veterinary Medicine, Vietnam National University of Agriculture (VNUA), Trau Quy-Gia Lam, Hanoi, Vietnam*
[4]*Department of Physics, Thai Nguyen University of Technology, Thai Nguyen City, Vietnam*
[5]*Department of Electronics and Communication, University of Information and Communication Technology (ICTU), Thai Nguyen City, Vietnam*
[6]*Faculty of Materials Science and Engineering (MSE), Phenikaa University, Hanoi 12116, Vietnam*

Correspondence should be addressed to Nguyen Le Nhat Trang; trang.nguyenlenhat@phenikaa-uni.edu.vn and Anh-Tuan Le; tuan.leanh@phenikaa-uni.edu.vn

Received 3 February 2021; Revised 19 April 2021; Accepted 29 April 2021; Published 8 June 2021

Academic Editor: Duong Tuan Quang

In this work, an eco-friendly approach for the synthesis of biogenic silver nanoparticles (bio-AgNPs) using botanical extracts in combination with an electrochemical process was carried out. We employed three types of plant extracts, including green tea leaf (GTE), grapefruit peel (GP), and mangosteen peel (MP) extracts to successfully synthesize the bio-AgNPs and optimized the experimental conditions aiming to get the highest synthetic yield. The formation of bio-AgNPs was monitored by UV-Vis spectroscopy via a surface plasmon resonance (SPR) band at about 420–430 nm. Transmission electron microscope (TEM) showed their spherical shape with the size range within 23–55 nm. While X-ray diffraction (XRD) analysis described in detail the crystalline structure of the bio-AgNPs with a face-centered cubic crystal lattice of metallic silver. The chemical bonding and elemental compositions of the bio-AgNPs were determined by Fourier Transform Infrared (FTIR) spectroscopy, in which organic compounds in the natural extracts not only acted as effective reductants but also capping agents for the fabricated bio-AgNPs. The prepared bio-AgNPs exhibited high stability and excellent dispersion for about four months. Based on the linear relationship between obtained SPR band intensity of bio-AgNP GTE in the presence of Fe (III) and concentration of Fe (III) ions, our bio-AgNP GTE can be used to develop a highly selective colorimetric sensor for the determination of Fe (III) ions within a linear range from 1 to 25 μM. According to that, the limit of detection (LOD) was recorded at approximately 0.532 μM, and the quantitative limit (LOQ) was calculated to be 1.77 μM. A detection mechanism was proposed through redox reactions between bio-AgNP GTE and Fe (III) ions. More interestingly, this method was successfully applied for the determination of Fe (III) ions in a lake water sample with percentage recovery of 107-150% and high reproducibility (RSD = 1.49%).

1. Introduction

Nanoscience is an emerging multidisciplinary field facilitating the design development, improvement, and potential application of nanomaterials. Metallic nanoparticles (NPs) exhibit many unique features such as high aspect and surface area/volume ratios, novel electromagnetic, chemical, and optical properties compared to those of the bulk metal [1–3]. Among them, AgNPs have been regarded as promising candidates for various studies in nanoscience due to their unique properties including antibacterial [4, 5], antifungal [6, 7], antiviral [8], antioxidant [9, 10], and anticancer [11] activities contributing to developing applications in wound healing, dentistry, and biomedicine [6, 12–16]. Besides, AgNPs have also been reported as a new generation of catalysts for organic chemistry [17] and highly sensitive bio/-chemosensors [18]. Those attractive applications lead to a growing demand for novel fabrication types of AgNPs.

The AgNPs in different sizes and shapes have been synthesized for several years by a series of various techniques, for example, physical, chemical, and biological ones [19]. Even though some physical and chemical methods have been successfully reported for producing the AgNPs in aqueous stable state in controlled sizes and shapes [20–24], many of them have required extreme synthetic conditions such as high temperature and pressure, which might be expensive and tedious for material costs. Moreover, the use and release of hazardous chemicals and solvents are potential risks for the environment and human health [25, 26]. Hence, there is a growing need to investigate alternative approaches which are more environmentally and economically feasible to synthesize these NPs. Biogenic methods of fabrication of AgNPs involving bacteria, fungi, or plant extracts might answer this demand. In recent years, plant extracts have been the most favorable. Stems, leaves, roots, flowers, or fruits of plant species have been employed to synthesize functional nanomaterials applying green chemistry technology [27–30]. In comparison to other biological routes, plants exhibit more accessible availability, more convenient preparation, better cost-effectiveness, and more comfortable scaling up production [31–33]. Besides, in the presence of plant extracts, the rate of metal ion reduction is also higher compare to that of microorganisms [33]. In general, various metabolites and reductive biomolecules (e.g., polyphenols, tannic acids, flavonoids, and terpenoids) in the plant extracts act as bioreductants to reduce Ag^+ ions into metallic Ag^0 simultaneously. They also play the role of stabilizers to prevent the conglomeration of bio-AgNPs [27, 34]. Furthermore, using polyphenols, flavonoids, terpenoids, amino acids, vitamins, etc. from plant extracts as capping agents can improve the characteristics of newly fabricated NPs [15, 35, 36], which is promising to develop advanced technological applications.

Previously, bio-AgNPs have been synthesized by using different plant extracts as reducing agents. Aloe vera leaf extract (*Aloe vera*) was employed to prepare bio-AgNPs with the size of 70–192 nm from $AgNO_3$ solution using the hydrothermal method [37]. In 2013, Geethalakshmi and Sadara described the one-step synthesis of bio-AgNPs based on incubation of aqueous solutions containing $AgNO_3$ and a solution of saponin isolated from *Trianthema decandra*. They obtained the NPs rapidly with the size of 17.9–59.6 nm [38]. Besides, tea leaf extract has been a popular candidate to develop different methods on this approach. Many kinds of evenly dispensed bio-AgNPs with the various diameters (from 20 to 90 nm) have been prepared using this kind of extract [39–42]. In a recent study, Sökmen et al. were successful in designing to generate the bio-AgNPs with green tea extract in citric acid 0.1 M. The bio-AgNPs of about 15 nm in diameter were obtained in a microwave-assisted production system after the addition of $AgNO_3$ solution [39]. More recently, spherical bio-AgNPs were produced from $AgNO_3$ using green tea extracts in a basalt medium. The newly fabricated NPs exhibited low toxicity to mammalian cells but antibacterial effects on several pathogenic bacteria [42]. Those studies resulted in successful biogenic manufacture of AgNPs with excellent applications; however, they still involved several chemicals, especially silver salts ($AgNO_3$) in excess, which is a source of Ag^+ that is toxic to mammalian cells [43], so it is harmful to human and also the ecosystem. Thus, researchers still keep trying to investigate more "green" methods for the synthesis of bio-AgNPs.

From an analytical point of view, iron (Fe) is essential for living bodies in all biological kingdoms. It is necessary for many physiological processes such as oxygen transportation, electron transfer, and regulation of cell growth and differentiation [44, 45]. However, at the evaluated level, it becomes toxic as excess free iron in cells, which can produce reactive oxygen species (ROS) arising from interconverting between Fe^{3+} and Fe^{2+}. Moreover, there is no active mechanism to excrete ion from the body. As a result, excess iron often leads to the damage of different organs, especially the heart, liver, and bone [46]. Nowadays, an increasing amount of ferric ion from domestic, agricultural, and industrial activities has been accumulated in the aqueous ecosystem, while water treatment plants are unable to eliminate it completely. As a result, even our drinking water and food source have been polluted with ferric ions. The World Health Organization (WHO) has set the "Guidelines for Drinking-Water Quality" of Fe (III) ions as 2 mg/mL (36 μM) [47]. Hence, it is pertinent to develop a sensitive method to determine Fe (III) ions in aqueous systems, biological, or food specimens [48]. Definitely, Fe (III) ions can be detected and quantified accurately by routine analytical techniques including atomic absorption spectroscopy (AAS), in-mass mass spectrometry, and inductively bonded plasma emission spectroscopy and liquid chromatography high performance (HPLC) [49–54]. However, these methods require expensive instruments, technical expertise, and elaborate sample preparation. Recently, the colorimetric detection method using plasmonic NPs has attracted the attention of global researchers due to its simplicity, high sensitivity, and fast response. Moreover, this method is capable to be developed into a compact and portable sensing system for practical applications. On the other hand, gold and silver have been known as noble metal NPs possessing impressive optical properties, which have been the most-used materials for this approach of Fe (III) detection. The gold nanoparticle was employed in a 2011 study to detect Fe^{3+} in the linear range of 10 μM–60 μM and

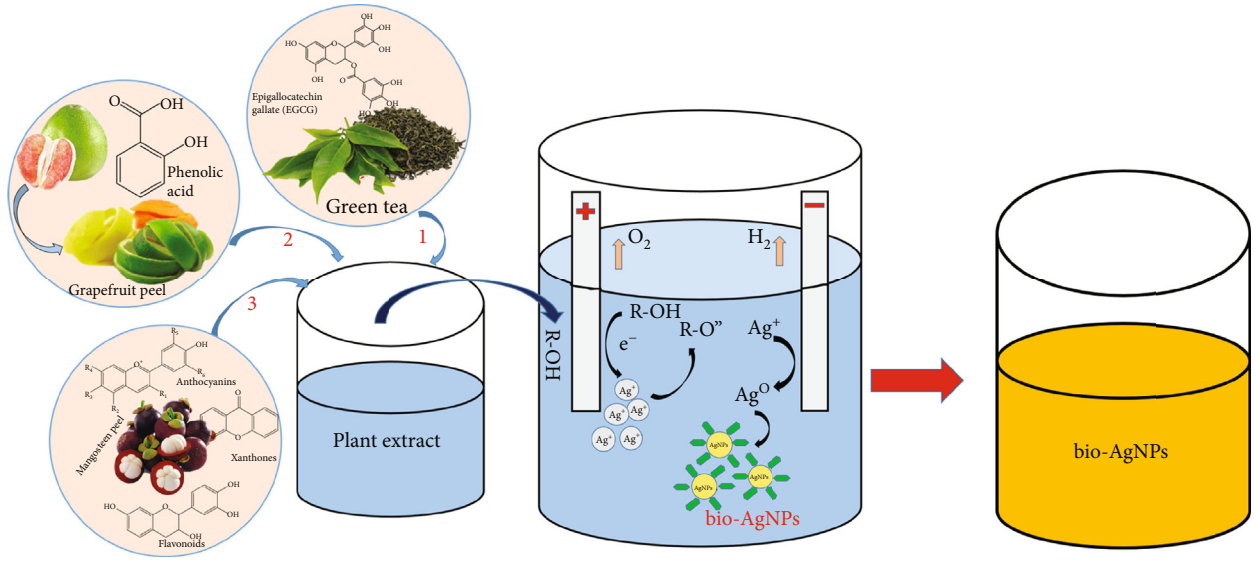

Figure 1: Extraction process combined with the electrochemical method to fabricate bio-AgNPs from plant extracts.

detection limit LOD = 5.6 μM [55]. In 2015, Gao et al. fabricated and utilized N-acetyl-L-cysteine stabilized AgNPs for detecting Fe (III) ions in the linear concentration range from 80 nM to 80 μM, corresponding to LOD = 80 nM [56].

In this study, we proposed a new method to synthesize a bio-AgNP solution using extracts from three natural plant sources including green tea leaves, grapefruit peel, and mangosteen peel in combination with an electrochemical technique using a metallic silver bar to produce Ag^+ ion source. This is a new "green" technology that is highly efficient in generating metallic nanomaterials in controlled shapes and sizes and can be easily scaled up for a large amount of products. The conventional electrochemical synthesis of AgNPs was performed by allowing an electric current to flow between two electrodes (cathode and anode) in an electrolyte solution. Here, we used plant extracts as electrolyte solutions. *Epigallocatechin gallate* in green tea leaves [40, 41]; *phenolic acid* in grapefruit peel [57]; and four main phenolic compounds including *xanthones*, *flavonoids*, *anthocyanins*, and *tannins* in mangosteen peel [58, 59] played the roles of reducing agents to reduce Ag^+ ions into Ag^0 as well as a surface stabilizer to help the newly synthesized nanoparticles to be well-dispersed and stable in the aqueous environment. The whole experiments were carried out under ambient conditions, using natural plant extracts as alternatives for metal salts and organic solvents. Therefore, this method is more simple, eco-friendly, and high cost-effective to synthesize the bio-AgNPs. The fabricated bio-AgNPs were characterized via different techniques, for instance, transmission electron microscopy (TEM), X-ray diffraction (XRD), and Fourier Transform Infrared (FTIR) spectroscopy to determine their size, shape, and composition. According to that, to take advantage of the potential optical properties of these novel bio-AgNPs, the development of colorimetric sensing systems has been more focused, so here, we described a bio-AgNP-based ultrasensitive detection of Fe^{3+} ion in aqueous solutions. By adding Fe (III) ions, the color of the bio-AgNP solution rapidly changed and the color difference could be observed by the naked eye. It is undeniable that the bio-AgNP solution is an ideal probe for a simple, fast, sensitive, and environmentally and economically effective method of Fe (III) detection.

2. Experimental Procedures

2.1. Chemicals. Two silver rods with a height of 70 mm and a diameter of 2 mm are used as electrodes. Ammonium hydroxide (NH_4OH, 25%), nitric acid (HNO_3, 63%), sulfuric acid (H_2SO_4, 98%), hydrochloric acid (HCl, 37%), iron (III) nitrate ($Fe(NO_3)_3$, 99%), copper (II) sulfate ($CuSO_4$,99%), potassium carbonate (K_2CO_3, 99%), zinc nitrate($Zn(NO_3)_2$, 99%), nickel (II) nitrate ($Ni(NO_3)_2$, 99%), cobalt (II) chloride ($CoCl_2$, 99%), and sodium chloride (NaCl, 99%) were obtained from Shanghai Chemical Reagent.

2.2. Preparation of Plant Extracts. Three kinds of botanical extracts from the green tea leaf, grapefruit peel, and mangosteen peel were prepared. Raw materials (with the weight mentioned below) were collected and washed by water and, then, dried naturally under shade. Next, they were cut into fine pieces. After that, each kind of plant material was immersed in 100 mL distilled water at 80°C. The mixture was incubated at 60°C for 20 minutes upon constant stirring to extract organic compounds from plant materials. From each mixture, 80 mL of plant extract was obtained and diluted using 420 mL of distilled water for the following experiments.

2.3. Electrochemical Synthesis for Bio-AgNPs Combined with Plant Extracts. The proposed process for the synthesis of bio-AgNPs is based on a two-electrode setup system in combination with the controlled addition of natural plant extracts (see Figure 1). The electrochemical experiments were carried out in a 500 mL beaker filled with diluted botanical extracts as described in the part of experimental procedures. Two rods of bulk Ag (70 mm in height × 2 mm in diameter) were

employed as the anode and the cathode and placed vertically face-to-face 3 nm apart. The two electrodes were mechanically polished and washed with distilled water to eliminate oxides on the surface. Electrolysis was performed at room temperature upon magnetic stirring. The voltage and time for the electrochemical process will be mentioned below. During electrolysis, the solution color gradually changed from yellow to finally to yellowish-brown, suggesting the formation of bio-AgNPs.

2.4. Optimization of Experimental Conditions for Electrochemical Synthesis of Bio-AgNPs Using Plant Extracts. To optimize the electrochemical synthesis of bio-AgNPs with the presence of plant extracts, three factors, including the amount of extract, reaction time, and DC voltage setup during electrolysis, were investigated to evaluate their effects on the fabrication of bio-AgNPs.

With group 01, electrochemical synthetic bio-AgNPs using green tea extract (bio-AgNP GTE), the weight of dry green tea was varied from 0.5 to 2 g, and the extract was employed for electrolysis in 30 minutes at a constant voltage of 12 V. After obtaining the optimal amount of green tea, this amount of botanical material was used to conduct the following experiments during varied periods of fabrication time, from 15 to 45 minutes, at a voltage of 12 V (Table S1).

With group 02, electrochemical synthesis of bio-AgNPs using grapefruit peel extract (bio-AgNP GP) was also performed under different experimental conditions. First, from fresh grapefruit peel with the weight in a range from 2.5 to 4.5 g, the extracts were prepared as an electrolyte for electrolysis in 30 minutes at the voltage of 12 V. The optimal amount of grapefruit peel was then applied for other electrochemical syntheses in 30 minutes, in which the DC voltage was the variable (6–16 V). Finally, using the optimal amount and voltage, electrolysis was carried out in different periods (20–45 minutes) to optimize this factor (Table S2).

Similarly, for group 03, electrochemical synthesis of bio-AgNPs using mangosteen peel extract (bio-AgNP MP), we also conducted experiments to evaluate the influence of amount, voltage, and reaction time, on the formation of bio-AgNPs. First, fresh mangosteen peel weighted from 3 to 11 g was employed for the preparation of electrolyte solutions for electrolysis performed in 30 minutes at a constant voltage of 12 V. Second, different voltages (8–16 V) were applied in the electrochemical process using the optimal plant exact as an electrolyte in 30 minutes. Finally, reaction time was also optimized using the same strategy, in which it varied in the range from 15 to 45 minutes (Table S3).

2.5. Colorimetric Detection of Fe (III) Ions. 0.5 mL of diluted bio-AgNP GTE, GP, and MP into 10 mL using 9.5 mL of distilled water was used as a primary testing sample. 1 mL of Fe (III) ion solution in the various concentrations ranges from 1 to 25 μM was introduced into the above solution. The mixtures were then shaken in 20 minutes using a shaker before the corresponding absorbance spectra were recorded by UV-Vis spectrophotometer. The experiment was repeated three times.

The LOD and LOQ were calculated through the following equations (Eqs. 1 and 2):

$$\text{LOD} = 3S/b, \quad (1)$$

$$\text{LOQ} = 10S/b, \quad (2)$$

where S is the standard deviation of the blank solution and b is the slope of the analytical curve.

2.6. Characterization Techniques. A Bruker D5005 X-ray diffractometer using Cu-K_a radiation ($\lambda = 0.154056$ nm) under a voltage of 40 kV and a current of 30 mA was employed to investigate the crystalline structure of the synthetic samples. The morphology and size of the bio-AgNPs were studied using a JEOL JEM 1010 transmission electron microscope (TEM) at an acceleration voltage of 80 kV and the Fourier transform infrared (FTIR, JASCO 6100) spectroscopy was obtained with the KBr pellet technique in the 4000–400 cm^{-1} spectral region and a resolution of 2 cm^{-1}, respectively. The value of pH was measured by pH meters PH1200, Horiba, Japan. The UV-Vis absorbance spectra were recorded using an HP 8453 spectrophotometer, and 10 mm path length quartz cuvettes were used for the measurement.

3. Result and Discussion

3.1. Research on the Formation of Bio-AgNPs through the Electrolysis Method in the Presence of Plant Extracts

3.1.1. Optimization of the Electrochemical Process for the Synthesis of Bio-AgNPs Using Plant Extracts. The color change of the botanical extract solutions during electrolysis is the first signal of the successful syntheses of bio-AgNPs. In the experiments using the green tea extract or the grapefruit peel extract, the solutions gradually turned from pale yellow to yellowish. With the samples using mangosteen peel extract, the solution color changed from red to yellow-brown. The color change before and after synthesis can be considered to the Surface Plasmon Resonance (SPR) property of bio-AgNPs [60]. The UV-visible spectra of bio-AgNPs were examined after each experiment of synthesis. The value of λ_{max} was determined and compared to investigate the optimal conditions for the electrochemical synthesis of bio-AgNPs. As mention in the part of experimental procedures, we examined three factors, including the amount of extract, reaction time, and DC voltage.

With group 01, as-synthesized bio-AgNPs using green tea extract (bio-AgNP GTE), the first parameter studied was the weight of green tea. Reactions were independently performed employing different amounts of dry green tea in the range from 0.5 to 2 g. As illustrated in Figure S1a, an SPR band was easily seen in the range of 420–450 nm for the bio-AgNPs synthesized using different amounts of green tea, which is consistent with the characteristic range of λ_{max} for AgNPs [60]. Moreover, the intensity of the SPR band of bio-AgNP GTE increased with an increase in the weight of the raw botanical material, corresponding to the darker color of the solution towards yellowish-brown. Nevertheless, when using 2 g of green tea, after electrolysis, the solutions turned greenish-gray and the intensity of the SPR band significantly decreased, in comparison to other

samples. It may be explained by the aggregation of formed bio-AgNPs in the solution.

From visual observation of the UV-Vis spectra as well as the color of the solution after electrolysis, the most appropriate weight of green tea was found that should be used for extraction and biogenic synthesis of bio-AgNP GTE. Using 1 g of green tea for the synthesis, we obtained a sharp SPR band at 420 nm, corresponding to the yellowish-brown color of the solution. Furthermore, increasing the mass of green tea from 0.5 to 1 g resulted in the rise in SPR intensity, as well as a red-shift, which is attributed to increasing the grain size of bio-AgNPs. It was also confirmed by the characteristic color change of bio-AgNPs. Therefore, we propose that the optimal amount of green tea for the preparation of bio-AgNPs is 1 g in this study.

Employing the optimal mass of green tea, we examined the influence of electrochemical time on the synthesis by performing the bio-synthesis in different reaction times to find the most appropriate one. As shown in Figure S1b, lengthening the reaction time led to the increase of the SPR band, corresponding to the change of the color toward brown. After 45 minutes of electrolysis, the SPR band reached the highest intensity with the sharpest peak at 420 nm. This improvement might be due to the increase in the concentration of NPs in the solution. In consequence, the optimal conditions for electrochemical synthesis of bio-AgNPs using green tea extract are using 1 g green tea for extraction. The electrolysis should be carried out in 45 minutes at a constant voltage of 12 V.

Concerning Group 02 of as-synthesized bio-AgNPs using grapefruit peel extract (bio-AgNP GP), we investigated all three factors to optimize the conditions for the biosynthesis. Different amounts of fresh grapefruit peel were employed for extraction, and the extracts were then used as an electrolyte solution for electrolysis. An SPR band of about 430 nm, which is characteristic of bio-AgNPs, was observed in every sample. Moreover, the intensity of the SPR band of bio-AgNP GP was enhanced by adding more grapefruit peel, from 2 g to 4.5 g, corresponding to the color change from yellow-brown to dark-brown (Figure S2a). Among those UV-Vis spectra, the sample using 2.5 g grapefruit peel exhibited the sharpest SPR peak without broadband within 500–600 nm region and yellowish-brown color, showing the uniform formation of bio-AgNP GP. Therefore, this amount of grapefruit peel was chosen for the following experiments.

Similarly, different DC voltage and reaction times were also examined. To evaluate the effects of applied voltage on the bio-AgNP formation, we applied the variation of electrolytic voltage in the range of 6–16 V (Figure S2b). At low voltage such as 6 V and 8 V, there was no characteristic band for bio-AgNP GP. At higher voltage, from 10 V, we started observing absorption bands. However, at the voltage of 10 V, 14 V, and 16 V, the absorption spectra showed a band at around 400 nm and a large shoulder at about 500 nm, while at the voltage of 12 V, a sharp band was observed at 430 nm, which is characteristic for bio-AgNPs. Therefore, it was evident that 12 V is the optimal voltage for the electrochemical synthesis of bio-AgNPs using grapefruit peel.

Figure S2c demonstrates the effect of the electrochemical time tested on the electrochemical synthesis at 12 V, using the extract from 2.5 g grapefruit peel as an electrolyte. Although lengthening the reaction time resulted in the increase in the intensity of the absorption bands in UV-Vis spectra, only the spectrum of the sample of 30 minutes exhibited the characteristic SPR band for bio-AgNP GP at 430 nm. Thus, the optimal reaction time for electrochemical synthesis of bio-AgNP using grapefruit peel extract is 30 minutes.

To sum up, the optimal experimental condition for the synthesis of bio-AgNPs from grapefruit peel extracts through the electrochemical process is the usage of 2.5 g grapefruit peel for extraction, an electrolytic voltage of 12 V, and a reaction time of 30 minutes.

A similar sequence of experiments was performed using mangosteen peel extract as the electrolyte solution for the electrochemical synthesis of bio-AgNPs MP to optimize those three factors. Several amounts of fresh mangosteen peel, from 3 to 11 g, were employed for extraction. Being different from the other extracts, the color of mangosteen peel extract is red in color, so during the electrochemical synthesis, the color gradually switched from red to reddish-brown and then dark brown. However, the SPR band at about 420 nm further confirmed the formation of bio-AgNP MP (Figure 2(a)). The increase in weight of the fresh mangosteen peel led to an increase in the intensity of the SPR band of bio-AgNP MT. Moreover, a red-shift was recorded in the UV-Vis spectra of bio-AgNP MP synthesized using a larger amount of mangosteen peel extract compared to the one using a lower amount. It might be due to the increase in particle size, exhibiting via the darker color of the bio-AgNP MP solution. Using 5 g of mangosteen peel, we obtained a sharp SPR band at 420 nm. Using a larger amount of peel such as 7 or 9 g did not significantly improve the band intensity. Employing 11 g of mangosteen peel led to a rise in the intensity of the SPR band; however, the appearance of a shoulder at around 510 nm might correspond to the aggregation of AgNP MP in the solution. Therefore, 5 g of mangosteen peel was chosen as the optimal mass of botanical material for the following experiments.

Voltage is also an important factor that impacts the formation of bio-AgNP MP during electrochemical synthesis. As shown in Figure 2(b), starting from 10 V, a SPR band was observed at around 420 nm. Clearly, the increase in the voltage led to improve significantly intensity of the SPR band. Compared to the other voltages, the sample using 12 V and 14 V for electrolysis exhibits a sharp band without any large shoulder. We select the voltage of 12 V for the following experiments.

Reaction time is the last parameter that we studied to optimize experimental conditions for electrochemical synthesis of bio-AgNPs using mangosteen peel extracts. Figure 2(c) demonstrates that the intensity of the SPR band increased with the lengthening of reaction time as longer reaction time might have allowed more Ag^+ to come into the solution and be reduced to Ag^0 to form metallic NPs. After 30 minutes of electrolysis, the solution obtaining exhibited a sharp SPR band at 420 nm. Extending the reaction time to 40 minutes did not significantly improve the intensity of

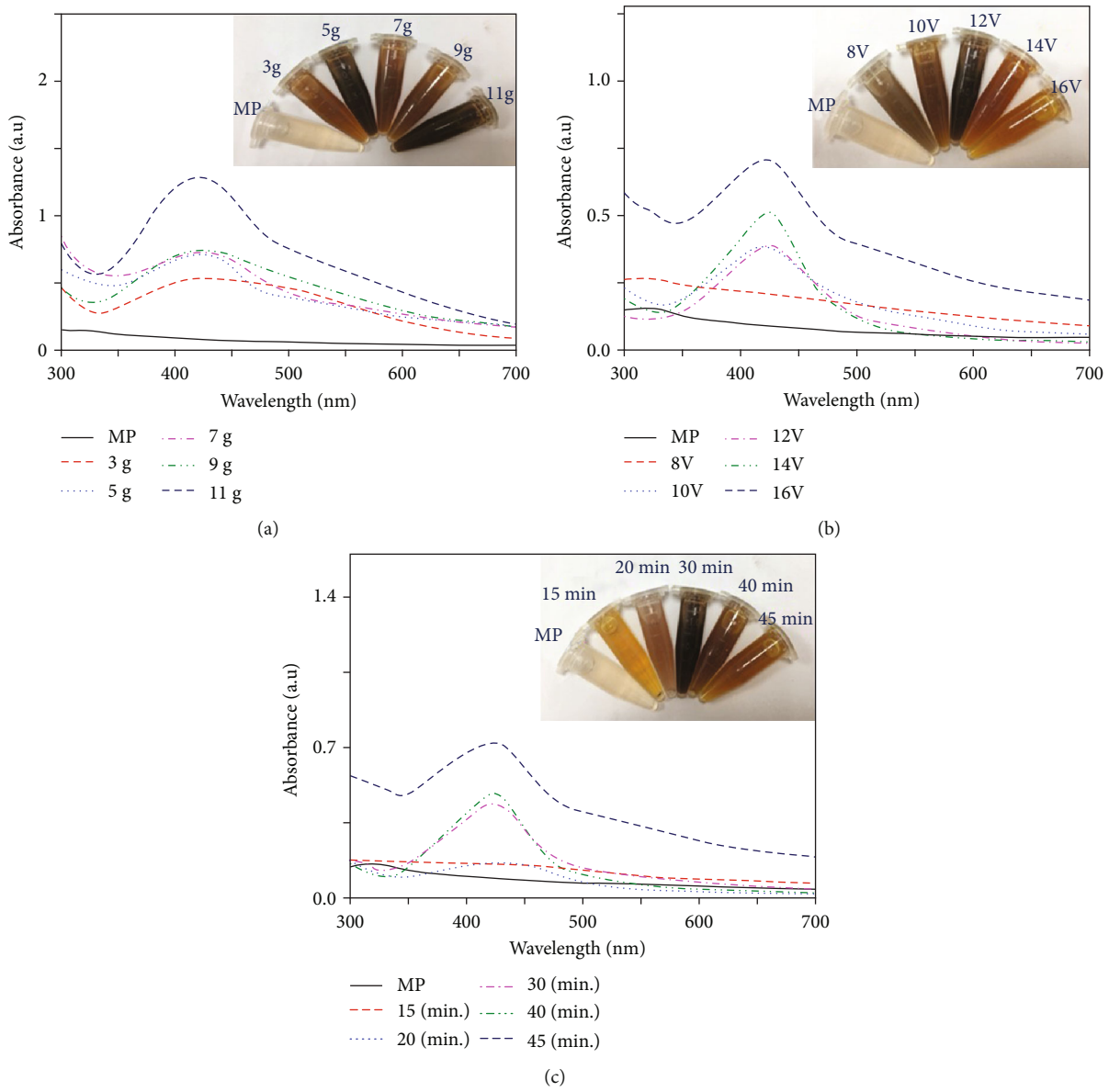

Figure 2: UV-Vis spectrum of bio-AgNP MP using mangosteen peel extracts synthesized at different masses of mangosteen peel (a), the applied DC voltage (b), and time of synthesis reaction (c), respectively. Insert pictures of bio-AgNP MP with different experimental conditions.

the band. After 45 minutes, the intensity increased but the appearance of a shoulder at about 520 nm might be a signal of aggregation. Furthermore, the color of the sample after 30 minutes of electrolysis was the darkest, which might correspond to the highest concentration of bio-AgNP MP. Hence, the reaction time of 30 minutes was regarded as the most appropriate one for this kind of synthesis.

In summary, to synthesize bio-AgNP MP using mangosteen peel extracts through electrochemical technique, 5 g of the fresh peel should be used for extraction, and the electrolysis should be carried out in 30 minutes at a constant voltage of 12 V.

3.1.2. A Mechanism for the Formation of these Bio-AgNPs. The results obtained from the investigation for optimal experimental conditions suggested that the formation of bio-AgNPs was substantially influenced by the mass of the raw botanical materials. We expected that it also affects the composition of the fabricated bio-AgNPs.

Green tea leaf extract contains several water-soluble phenolic compounds such as catechin (C), epicatechin (EC), epigallocatechin (EGC), and epigallocatechin gallate (EGCG) [40]. In particular, catechins are the main phenols in green tea, which allows the silver ions to be strongly reduced and thus to form AgNPs [40]. The phenolic configuration and catechin content, as well as the quantitative extraction of the extract, can be determined by HPLC analysis as previously reported [61]. Based on the above results, a possible mechanism of the bio-AgNP formation in green tea extract was proposed in Figure 3. Upon application of voltage, OH^-

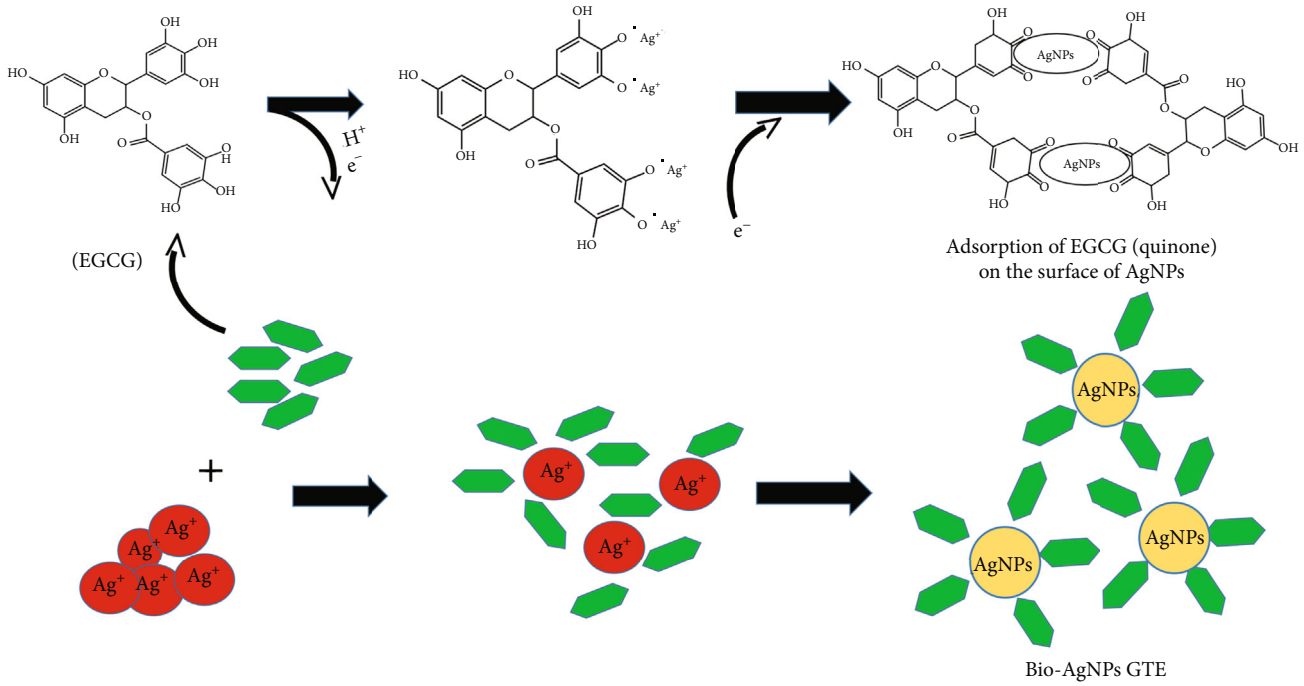

Figure 3: Mechanism of forming bio-AgNP GTE from green tea extract.

ions and Ag^+ ions were formed on the surface of the cathode and anode at the same time. Silver ions migrated from the anode migrate to the cathode, a part of Ag^+ ions was reduced to Ag^0. EGCG presents as the most-seen catechin, and it is also the most active component in green tea. EGCG consists of multiple phenolic hydroxyls, so it tends to eject the phenolic photon strongly. Hence, the presence of poly –OH groups in the structure explains why EGCG can transfer the photon to Ag^+ easily to form stable EGCG-AgNPs [41] (see Figure 3).

Figure 3 illustrates the possible mechanism of bio-AgNP GTE formation during the electrochemical process in the presence of EGCG from green tea extract. The first reaction represented proton ejection (one electron one-step oxidation-reduction mechanism), leading to the formation of Ag^0 and EGCG radical. In the following reaction, EGCG radical is immediately converted to a stable quinone. Ag^0 atoms aggregated together to form clusters, and then, they grow into bio-AgNPs. These NPs were coated by the phenolic compound EGCG to achieve a steady-state of NPs.

Grapefruit peel extract contains phenolic acid, while mangosteen peel extract contains several kinds of phenolic compounds. Thus, the formation of bio-AgNP MP also occurred in a similar mechanism as the flexible –OH groups of these polyphenolic compounds transfer their proton to reduce Ag^+ to Ag^0. Silver atom then aggregated together and became NPs coated by the phenolic compounds in the extracts (Figure S3).

3.1.3. Characterization Studies and Stability of Bio-AgNPs at the Optimum Conditions. Once bio-AgNPs were prepared using green tea extracts under the optimal conditions, the successful fabrication of bio-AgNPs was confirmed by TEM, XRD, and UV-Vis spectroscopy analyses, respectively. TEM images (Figure 4(a)—the inset) show the encapsulation of organic compounds in the plant extracts around the bio-AgNP GTE as well as the size and shape of the NPs. These images indicate that the bio-AgNP GTE were spherical in the size range of 20-30 nm, and they are evenly distributed within the shell of EGCG. The bio-AgNP GTE were dried and employed for XRD measurement (Figure 4(a)). The diffraction peaks at 38.1°, 44.4°, 63.8°, and 76.7° matched well to the (111), (200), (220), and (311) crystalline planes of the pure face-centered cubic (fcc) silver structure, respectively, which agrees with the reference JCPDS PDF 04-0783. In addition, no characteristic diffraction peaks of other phases (e.g., Ag_2O and AgOH) were detected in the two patterns, indicating high crystallinity of prepared bio-AgNP GTE. Also, XRD analysis further confirmed the formation of single-phase bio-AgNP GTE with high purity. Using the Debye-Scherrer equation, the average crystalline size of the bio-AgNP GTE was calculated to be approximately 23 nm, in accordance with TEM images.

The presence of polyphenols from green tea extracts on the NPs surface (Figure 4(b)) was demonstrated by Fourier-transform infrared (FTIR) spectroscopy data of bio-AgNP GTE. The broad and intense band at 3420 cm^{-1} were presented in the spectrum of bio-AgNP GTE, which was similar to that of the green tea extract. This peak was associated with the O–H elongated vibrations assigned -OH groups from polyphenols in green tea extracts such as catechins [62]. The band at 2913 cm^{-1} corresponded to elongated oscillations C-H and CH_2 of hydrocarbons [42]. The peak of 1630 cm^{-1} involved a prolonged C=O oscillation of the conjugate bonded to ketone, quinones, carboxylic acids, and esters [41, 42]. At 1392 cm^{-1}, there was a C-N elongated vibration of

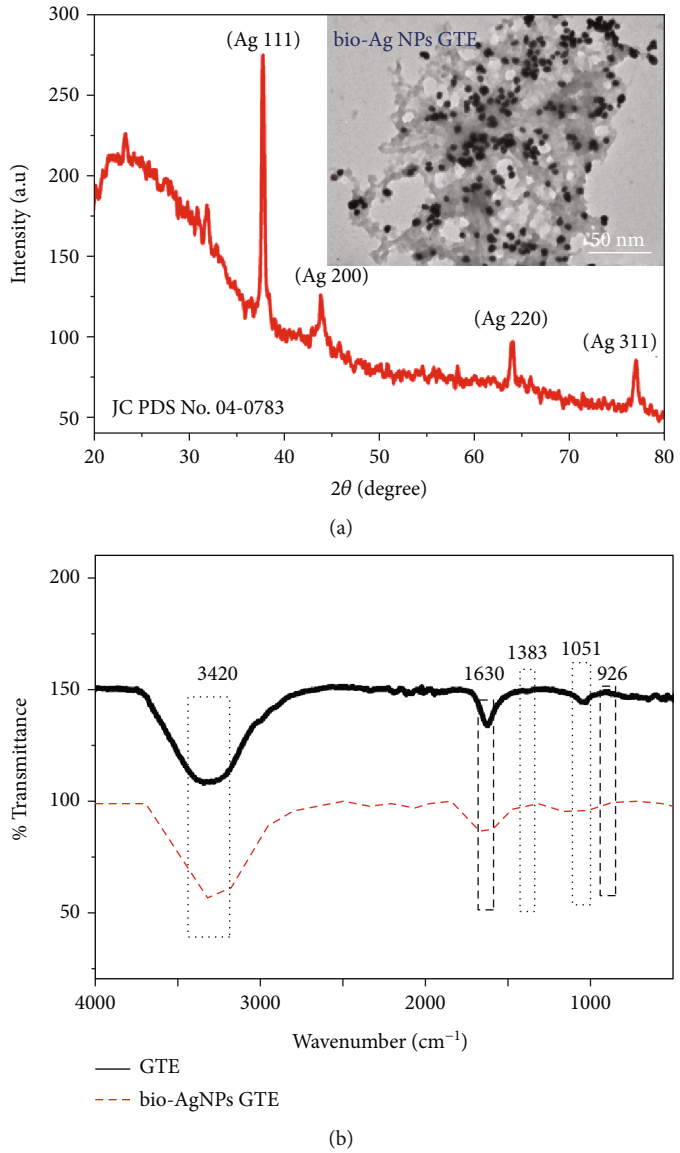

Figure 4: (a) XRD spectrum (inset: TEM image of bio-AgNP GTE). (b) FTIR spectrum of bio-AgNP GTE synthesized with green tea extract.

aromatic amines, indicating the presence of water-soluble EGCG. Furthermore, the band located at 1044 cm^{-1} was associated with C-O-C elongated vibration [63]. Most of the obtained results agreed with previous reports [64–66] and demonstrated the presence of the polyphenol in green tea extract as a protective agent on the bio-AgNP GTE surface, which also helped NPs to be well-dispersed in the aqueous environment.

Two other types of bio-AgNPs synthesized using grapefruit peel and mangosteen peel extracts were also characterized through XRD spectroscopy (Figure S4). Figure S4a demonstrates the XRD measurement of bio-AgNP GP prepared using grapefruit extract with diffraction peaks at 37.9°, 43.9°, 63.8°, 76.67°, and 82.7°, corresponding to (111), (200), (220), (311), and (222) crystalline planes of the pure fcc of bulk Ag (JCPDS PDF 04-0783). Besides, the Debye-Scherrer equation was used to determine the average crystal size of the formed bio-AgNPs in the range of 26 nm. Figure S4b shows the XRD data of bio-AgNP MP synthesized with mangosteen peel extract. Four diffraction peaks at 38°, 44.2°, 64°, and 76.6° were suitable for the (111), (200), (220), and (311) crystalline planes of the fcc silver structure, in accordance to JCPDS PDF 04-0783. The average crystal size of bio-AgNP MP was determined approximately 55 nm by using the Debye-Scherrer equation. In addition, no characteristic diffraction peaks of Ag_2O or AgOH were observed in the XRD results of all types of bio-AgNPs. These newly fabricated bio-AgNPs were confirmed to possess a face-centered cubic structure and high purity.

The stability of three types of bio-AgNPs synthesized using green tea, grapefruit peel, and mangosteen peel extract was also examined via visual observation and UV-Vis spectroscopy. Two months after synthesis, SPR bands of these bio-AgNPs showed an increase in intensity (Figure 5). This can be explained that the phytochemical compounds in the

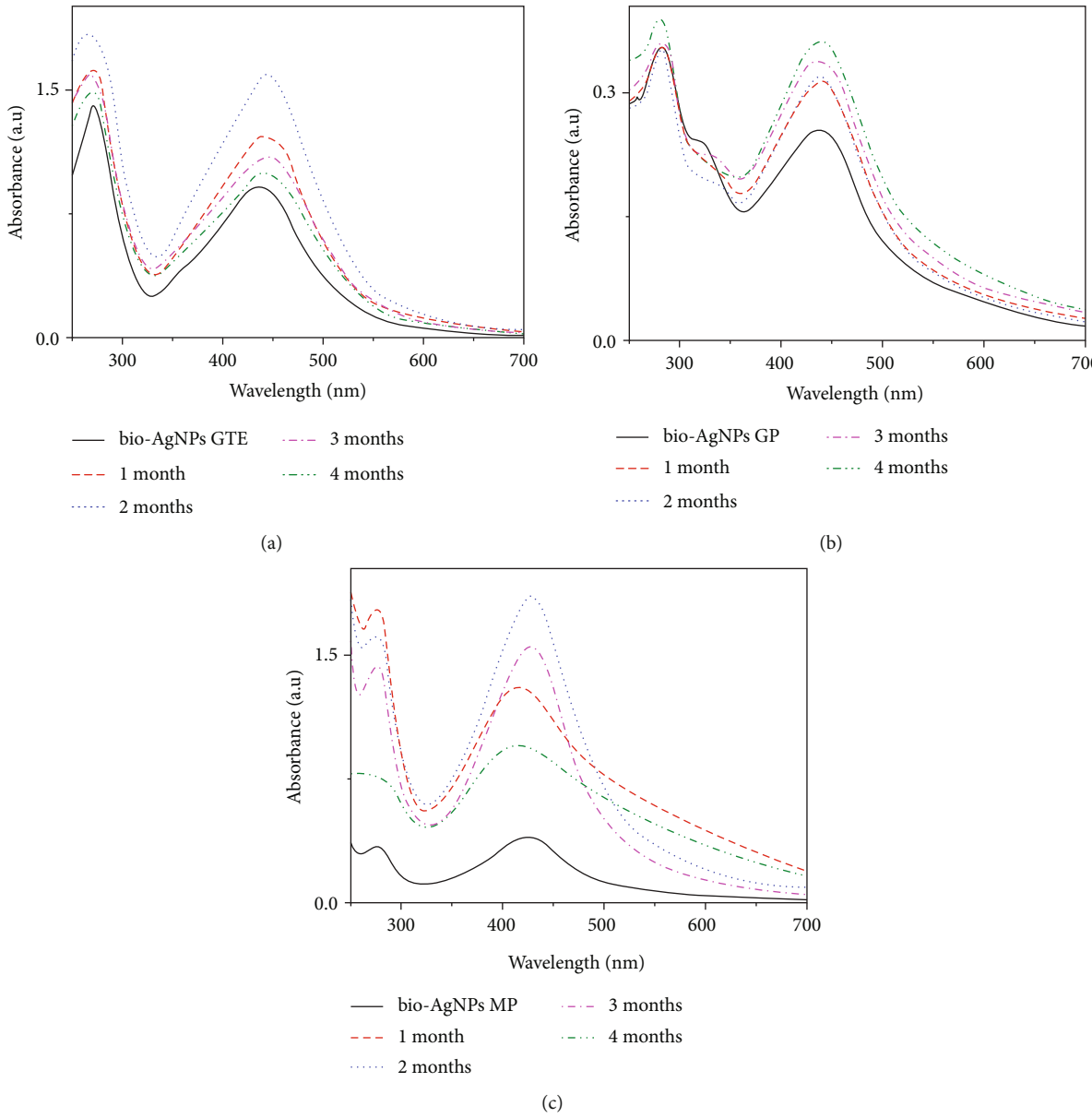

Figure 5: UV-Vis spectroscopy monitoring the stability of bio-AgNPs synthesized from green tea extract (a), grapefruit peel (b), and mangosteen peel (c) over time.

plant extracts were weak reducing agents, so Ag^+ formed by the electrochemical process was not completely reduced to Ag^0. Therefore, during this storage period, the reduction continued occurring, resulting in the enhanced concentration of bio-AgNPs, which caused the rise in absorption intensity. Two months later, the intensity of the SPR band of bio-AgNPs prepared using green tea and mangosteen peel extract tend to gradually decrease, corresponding to the faded color of the solutions. The reduction might stop. In addition, a sedimentation phenomenon was observed as NPs started aggregated. The percentage increase in the absorption intensity of bio-AgNPs over storage time was calculated in Table S4. Concerning bio-AgNPs fabricated with grapefruit peel extracts, even four months after synthesis, the SPR band intensity continued increasing, which could be the result of the continuous reduction.

3.2. Research on the Applicability of Bio-AgNPs towards Colorimetric Detection of Fe (III) Ions in Aqueous Solution. The bio-AgNPs synthesized from plant extracts were used with an aim to detect the colorimetric of metal ions. 1 mL of 25 μM Fe (III) ion was added to 10 mL of diluted bio-AgNP solutions (as described in the part of the experimental procedures). After being well-shaken, the color change of the solutions was observed by the naked eye. Besides, the obtained results from UV–visible spectroscopy exhibited the differences in their SPR band. By naked eye, it can see that only the bio-AgNP GTE synthesized from green tea extract showed the obvious color change in adding of Fe (III) ion, namely, the solution color of the bio-AgNP GTE changed from yellow to nearly colorless due to the agglomeration of created NPs. This change was then confirmed by UV-Vis absorption spectra with a drop-off in intensity along with a

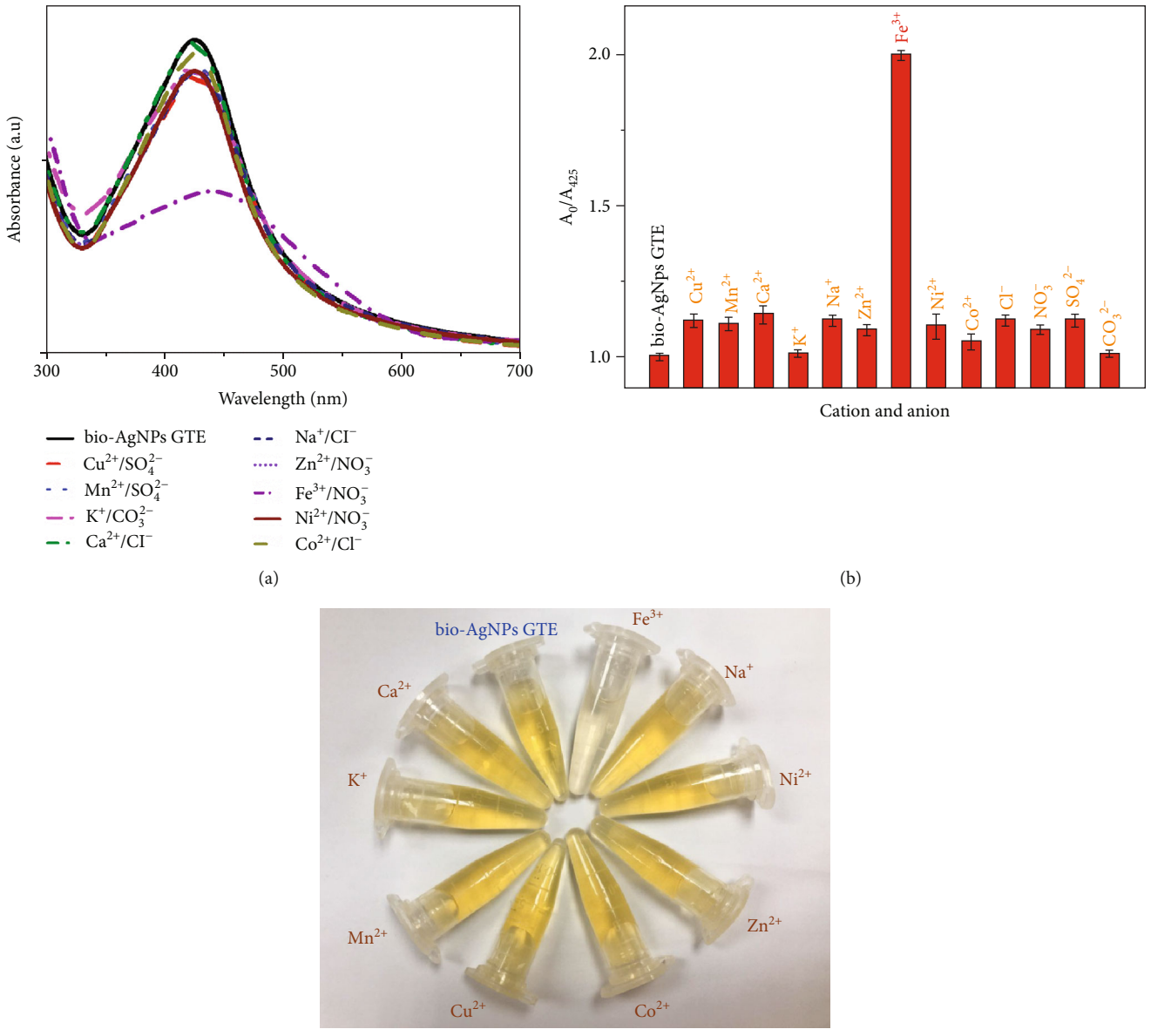

Figure 6: UV-Vis absorption spectra (a) of bio-AgNP GTE in the addition of 10^{-4} M ions (Co^{2+}, Cu^{2+}, Ca^{2+}, Zn^{2+}, Ni^{2+}, K^{+}, Na^{+}, Mn^{2+}, NO_3^{-}, Cl^{-}, and SO_4^{2-}) and 10 μM Fe (III) ions. (b) Comparison of the absorbance rate A_0/A_{425} of the bio-AgNP GTE with different ions. (c) A visual representation of the color change by using different ions.

red-shift of the SPR band (Figure S5a). In contrast, for bio-AgNP GP and bio-AgNP MP solutions, they did not exhibit any color change or shifting of absorption band when Fe (III) ions were added (Figure S5b, c). Hence, we chose the sample of bio-AgNP GTE for the following experiments to evaluate its selectivity of sensing metal ions.

3.2.1. Colorimetric Detection of Fe (III) Ions. In order to evaluate the selectivity of the colorimetric sensor, which was developed by bio-AgNP GTE for the detection of Fe (III) ions, we investigated the colorimetric response in the presence of a large amount of various interfering cations including (Co^{2+}, Cu^{2+}, Ca^{2+}, Zn^{2+}, Ni^{2+}, K^{+}, Na^{+}, and Mn^{2+}) and anion (NO_3^{-}, Cl^{-}, and SO_4^{2-}) with 10-fold excess concentrations. The change in UV-Vis spectra of bio-AgNP GTE solution with and without adding a pair of above cations and anions (10^{-4} M) were shown in Figure 6(a). It is evident that only the sample containing Fe (III) ions exhibited a significant band change as described above. Figure 6(b) compares the absorption rate (A_0/A_{425}) after adding different ions into the bio-AgNP GTE solution (A_0 and A_{425} represent the SPR peak intensities of bio-AgNP GTE solution and bio-AgNP GTE solution in the addition of ions, respectively, Table S5). This fact was reconfirmed by visual observation in Figure 6(c) as only the solution with the presence of Fe (III) ions was colorless with the aggregation of NPs, while

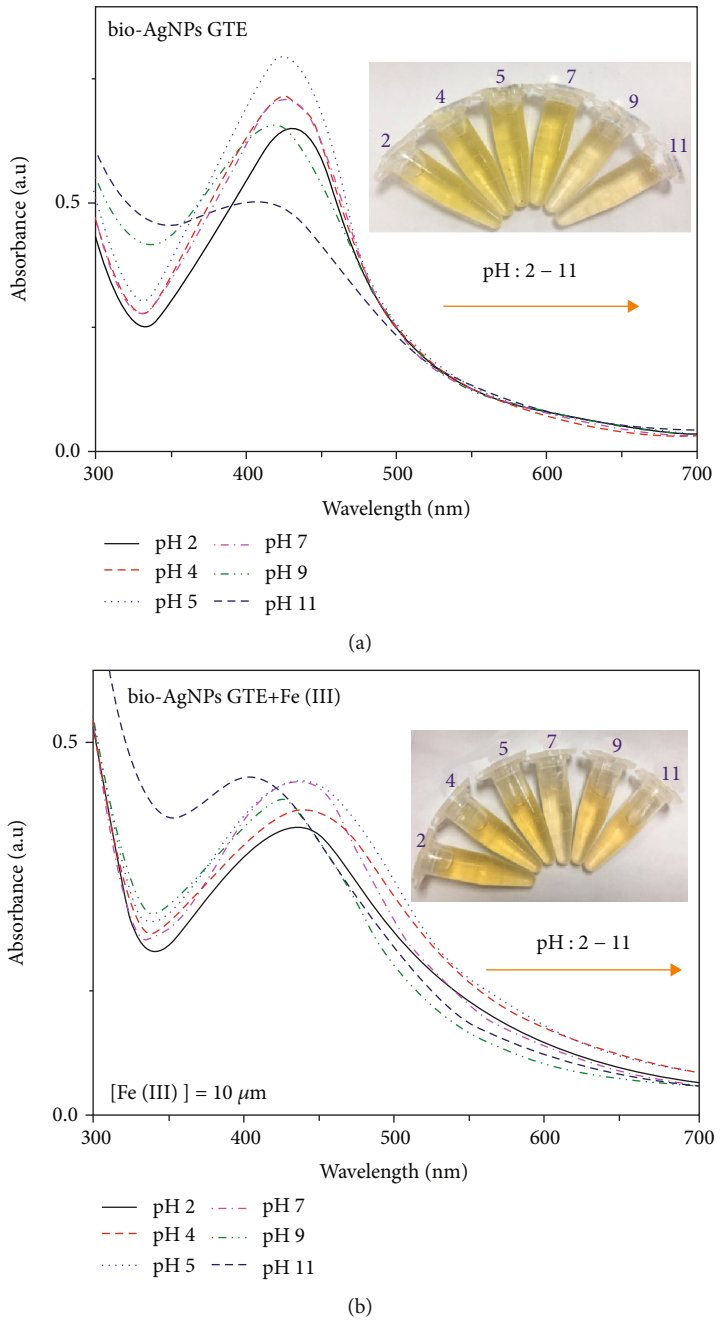

Figure 7: UV-Vis absorption spectra of bio-AgNP GTE without (a) and with (b) the presence of 10 μM Fe (III) ions in the pH range from 2 to 11. Inset (a) picture of bio-AgNP GTE with a pH between 2 and 11. Insert (b) picture of bio-AgNP GTE with a pH range of 2 to 11 in the presence of 10 μM Fe (III) ions.

the others remained yellow. These results state that the proposed bio-AgNP GTE-based colorimetric sensor is highly selective to Fe (III) ions.

The bio-AgNP-based colorimetric sensors were highly dependent on the pH of the solution. In the present study, the pH value can affect the interaction of Fe (III) ions with bio-AgNP GTE as well as the state of the functional groups surrounding the NPs. Therefore, different sets of experiments were performed using nitric acid (HNO_3) and NH_4OH to adjust pH in the range from 2 to 11. The UV-Vis absorption spectra of bio-AgNP GTE solution were observed in the absence and presence of 10 μM Fe (III) (see Figure 7). When without adding Fe (III), bio-AgNP GTE solutions were bright yellow at the pH in the range of 2–7. These samples also showed an SPR band at 425 nm. With high intensities of the SPR band, the bio-AgNP GTE exhibited high stability in the pH range of 4 to 7. Whereas, when the pH was larger than 7, the oxidation of bio-AgNP GTE occurred leading to a blue-shift of the plasmon peak, along with that the color of the solutions faded and turned into light reddish-yellow.

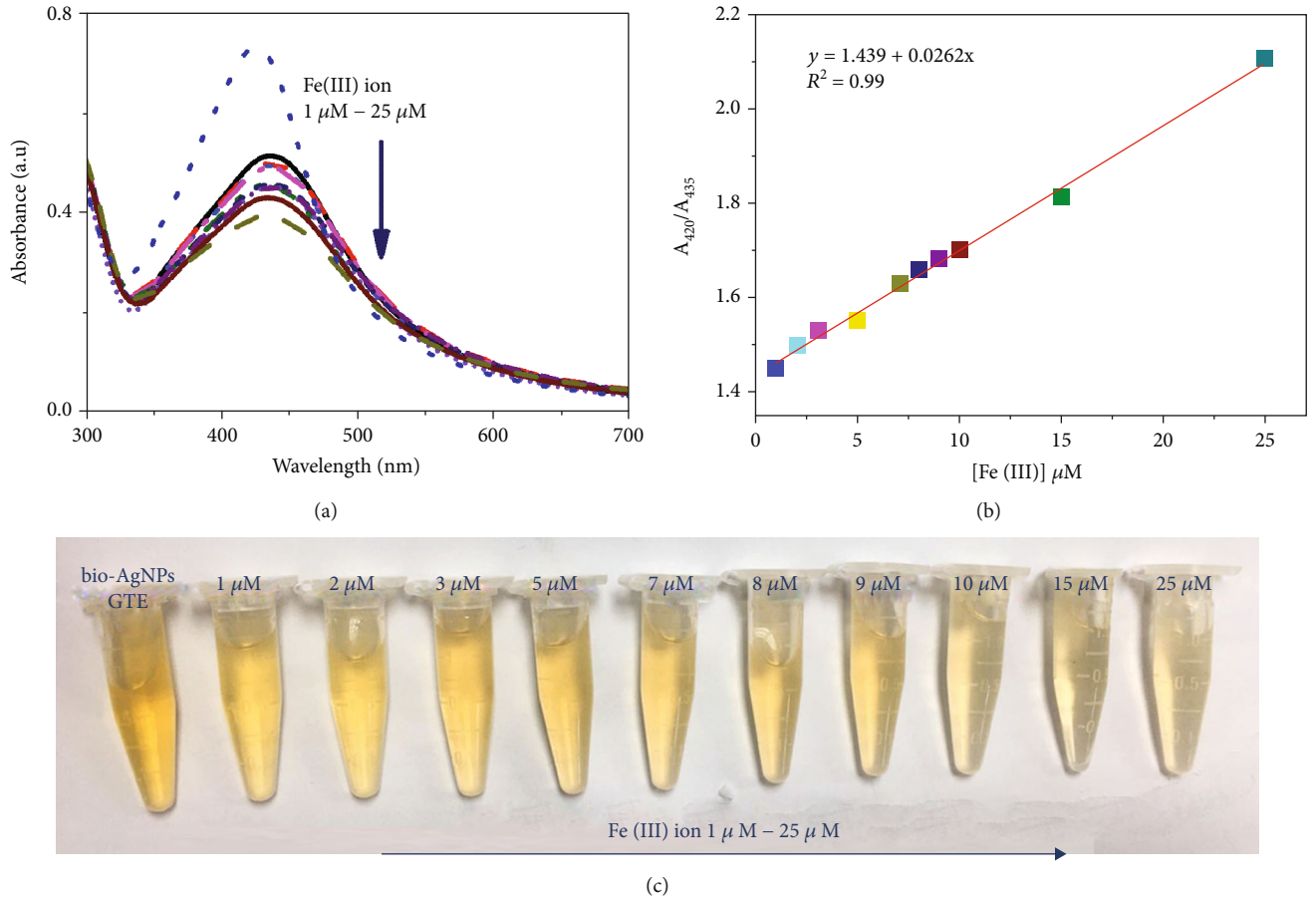

FIGURE 8: Spectroscopy absorption UV-Vis (a) and photographic image (c) of bio-AgNP GTE in the presence of Fe (III) ions at various concentrations determined at pH 7 (1-25 μM). (b) The plot of absorbance ratio (A_{420}/A_{435}) against the Fe (III) concentration range of 1-25 μM and its linear calibration curve (A_{420} and A_{435} is the absorbance of the ion bio-AgNP GTE with/without adding Fe (III) ions, respectively).

In the presence of Fe (III) ions, the color change was the most obvious at pH 7, and the change of absorbance (ΔA) was also largest at this pH value. Therefore, the suitable pH value for effective detecting Fe (III) ions using bio-AgNP GTE solution was 7.

To evaluate in more detail the analytical performance of the bio-AgNP GTE-based colorimetric sensor for the detection of Fe (III) ion in water samples, the sensitivity was assessed by investigating some important parameters including linear range, LOD, and LOQ values. The sensitivity for detection of Fe (III) ion was determined by adding different amounts of Fe (III) ions within the bio-AgNP GTE solution. The changes in absorption spectra were recorded through UV-Vis results (Figure 8(a)). In which, it observed the decrease in intensity of the SPR band when increasing Fe (III) concentration in the bio-AgNP GTE solution, along with a slight blue-shift as well as the expansion of the SPR band. Figure 8(b) depicts the linear relationship between the absorption rate (A_{420}/A_{435}) and the Fe (III) ions concentration within the range from 1 to 25 μM (Figure 8(c)) (A_{420} and A_{435} denote the SPR peak intensities of bio-AgNP GTE with and without Fe (III) ions, respectively) with the linear regression equation of $A_{420}/A_{435} = 0.0262\, C_{[Fe3+]} + 1.439$ and correlation coefficient of 0.99. The LOD of the bio-AgNP GTE-based colorimetric sensor was 0.532 μM, and the LOQ was estimated to be 1.77 μM.

Table 1 summarizes several reported methods relating to the detection of Fe (III) ions to compare with the one that we propose in this work. It is obvious that the bio-AgNP GTE-based colorimetric sensor has to be not the best one, but its LOD is still lower than several others. More importantly, it is a sensing system which was developed by the most "green" process with a completely plant-routed coating agent. Moreover, this system could detect Fe (III) ions within a relatively wide linear range and a low LOD that is competitive compared to other colorimetric sensors. More importantly, the LOD 0.532 μM obtained by bio-AgNP GTE-based colorimetric sensor is much lower than the value reported by WHO guidance for *Drinking-Water Quality* ~36 μM. This sensing platform can open up new opportunities to develop an ultrasensitive colorimetric probe to detect Fe (III) ions in aqueous systems.

To evaluate the practical applicability of the newly-developed colorimetric sensor, we employed the bio-AgNP GTE-based colorimetric sensor to detect Fe (III) in water collected from Van Quan Lake, Hanoi, Vietnam. Before starting

Table 1: Comparison of the proposed method using bio-AgNP GTE with some other methods investigated in the literature for detection of Fe (III) ions.

Functional nanomaterials	Capping agent	Detection mechanism	Linear range	LOD (M)	Ref.
AgNPs 6.55 ± 1.0 nm	N-acetyl-L-cysteine-stabilized	Colorimetric sensor	0.08-80 μM	80 nM	[56]
ZnSe quantum dots 4, 1 ± 0, 2 nm	Thioglycolic acid	Colorimetric sensor	0-50 mM	2.2 mM	[51]
AuNPs (26-30 nm)	Pyrophosphate ($P_2O_7^{4}$ -AuNPs)	Colorimetric sensor	10-60 μM	5.6 μM	[55]
AuNPs 100 nm	Cetyltrimethylammonium bromide (CTAB)	Raman spectroscopic	100-10000 ppb	100 ppb	[67]
Graphitic carbon 9 nm		Fluorescent sensor	2 nM-5 μM	2 nM	[68]
Graphene quantum dots. (GQDs) 3 nm	(1-butyl-3-methylimidazolium hexafluorophosphate ($BMIMPF^6$)	Fluorescent sensor	0-400 μM	7.22 μM	[69]
Graphene quantum dots (GQDs) 3.8 nm	Nitrogen-doped (N-GQDs)	Fluorescent sensor	1-1945 μM	90 nM	[70]
Graphene quantum dots (GQDs) (2-4 nm)	p-toluenesulfonate S-GQDs	Fluorescent sensor	0.01-0.70 μM	4.2 nM	[71]
Bio-AgNP GTE 23 nm	Epigallocatechin gallate (EGCG)	Colorimetric sensor	1-25 μM	0.532 μM	This work

the detection, the lake water samples were pretreated through Whatman® Grade 1 filter paper (11 μm) to filter out the large impurities. After that, different volumes of Fe (III) ion solution were added into the treated water sample and analyzed with the standard method. Figure S6 demonstrates that the SPR band of bio-AgNP GTE decreased when the concentration of Fe (III) ion increased. Lake water contained various microorganisms and minerals that might have affected the detection of Fe (III), but the bio-AgNP GTE-based sensor still exhibited high sensitivity.

Figure S7 presents the linear relationship as revealed by the obtained SPR intensity *vs.* Fe (III) concentration. The good linearity demonstrates the effective ability to sense Fe (III) ions in lake water. The impressive results were summarized in Table 2. The recoveries achieved about 107 to 150 with a relative standard deviation (RSD) within 1.49%. For the direct addition of only lake water, there is not a significant change in the absorption spectrum of the bio-AgNP GTE solution, so the concentration of Fe (III) in lake water is extremely low. These results demonstrate that our prepared bio-AgNP GTE-based colorimetric sensor possesses high practical applicability for Fe (III) ion detection in lake water, and it is promising to determine Fe (III) ions in other sources of real water.

3.2.2. Sensing Mechanism of Fe (III) Ions Using Bio-AgNP GTE Probe. In general, fluorescent NPs such as Au, Ag NPs are employed to detect some transition metal ions as such metal ions can interact with the NPs and quench their fluorescence [72, 73]. Besides, nonfluorescent NPs are used to generate colorimetric sensors to detect metal ions due to the changes in SPR band (i.e., intensity and red- or blue-shift) in the addition of metal ions. These changes might be due to the dissolution, the aggregation of NPs, and even be the formation of new core-shell NPs [74].

Table 2: Analysis of Fe (III) ions using bio-AgNP GTE-based colorimetric sensor in lake water.

Added (μM)	Determined (μM)	Recovery (%)	RSD (%)^n
2	3	150	0.7
8	8.6	107.5	0.42
14	16.1	115	1.49

To observe the existence of bio-AgNP GTE in the solution after adding Fe (III) ions, FTIR measurement and UV-Vis absorption spectra were used. Based on the FTIR spectrum, we see that there was a fluctuation of the -OH group at about 3400 cm^{-1} leading to the OH elongation band. The expansion of the absorption peaks was considered to the absorption of water into a prepared sample. The maximum stretching vibration at ~1630 cm^{-1} was assigned to C=O. Besides, the sharp absorption peaked at ~1051 cm^{-1} related to C-O-C elongated oscillation (Figure S8) [42]. Measurements showed no synthetic AgNPs formed after Fe (III) ions were added.

Based on the obtained results, a redox mechanism for colorimetric detection of bio-AgNP GTE (see Figure 9) was proposed. In the previous studies, they have shown the possibility of a redox reaction between bio-AgNP and Fe (III) ions [45, 51, 56]. When Fe (III) ions were added to the bio-AgNP solution, a redox reaction occurred between Ag^0 and Fe^{3+} ions, so bio-AgNP were oxidized and decomposed while Fe^{3+} ions were reduced to Fe^{2+} ions or Fe^0 atoms. This mechanism could explain the decrease of SPR band intensity of bio-AgNP GTE solution depending on Fe (III) concentration. The partial oxidation of bio-AgNP

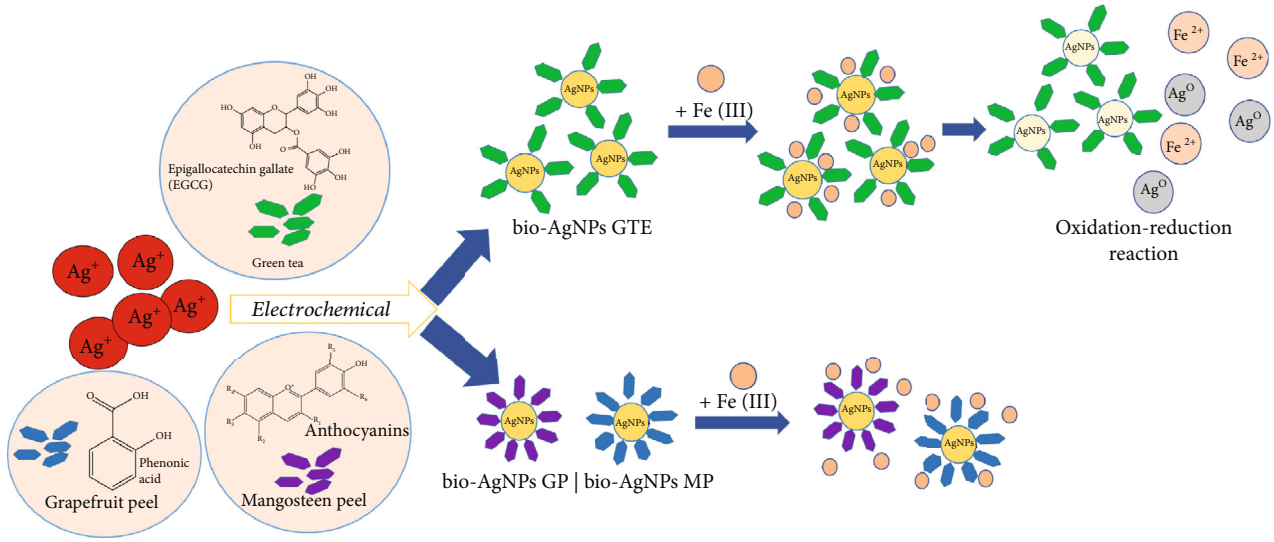

Figure 9: Possible mechanism of detecting Fe (III) ions using bio-AgNP GTE.

GTE in the low Fe (III) concentration might break the steady-state of the NPs, so they aggregated together and grew larger clusters, which resulted in the red-shift in absorption spectra and the agglomeration of NPs as described above.

Although Fe (III) ions were introduced to all of the three types of NPs synthesized using plant extracts in the same conditions, only bio-AgNP GTE solution became colorless. We assume that it might be due to the difference in the stabilizing agents of these bio-AgNPs. The phenolic acids in grapefruit peel or xanthones flavonoids, anthocyanins, and tannins in the mangosteen peel might have coated more tightly and seamlessly around the NPs, so it is more difficult for Fe (III) ions to interact with Ag^0 and degrade the NPs. As a result, Fe (III) ions do not discolor the bio-AgNP solutions prepared using these extracts.

4. Conclusions

In summary, the bio-AgNPs have successfully synthesized by a simple, cost-effective, and environmentally friendly method combining the electrochemical method and using natural extracts (green tea, grapefruit peel, and mangosteen peel) without using any additive chemicals. Inside, natural plant extracts played an important role as an effective reductant for Ag^+ ions as well as a great stabilizer for created bio-AgNPs for long-term storage. The influencing factors of various parameters such as input volume, electrochemical voltage, and fusion time have been optimized. As a result, we gave a data set of optimal parameters for each biosilver NPs synthesized from different extracts. Under optimal conditions, the obtained bio-AgNP-green tea was used as a colorimetric sensor for the most effective detection of Fe (III) ions. In the presence of Fe (III) ions, bio-AgNP GTE solution occurred color change from yellow to colorless while reducing absorption intensity and peak fluid absorption to long wavelength. The sensor has determined that the detection limit for Fe (III) ions was 0.532 μM and the LOQ was estimated to be 1.77 μM in the linear range 1-25 μM. The method was tested for the detection of Fe (III) ions in lake water with a percentage recovery of 107-150% and RSD = 1.49%.

Data Availability

Data are available on request.

Conflicts of Interest

The authors declare that they have no conflicts of interest.

Acknowledgments

This research was supported by the National Foundation for Science and Technology Development (NAFOSTED) through a fundamental research project (103.02.2019.01). We also thank the collaborative supports with XRD, TEM, UV-Vis, Electrochemical Synthesis measurements from the Institute of Materials Science-VAST, NIHE-Ministry of Health, and NEB Lab at the Phenikaa University Nano Institute (PHENA), respectively.

Supplementary Materials

Table S1: technical specifications for manufacturing bio-AgNP samples using green tea extract. Table S2: technical specifications for manufacturing bio-AgNP samples using grapefruit peel extract. Table S3: technical specifications for manufacturing bio-AgNP samples using grapefruit peel extract. Table S4: table showing the percentage (%) increase in the absorption intensity of bio-AgNP over time compared to the sample after synthesis. Table S5: the absorbance rate A_0/A_{425} of the bio-AgNP GTE with different ions. Figure S1: UV-vis absorption spectrum of bio-AgNPs synthesized using different amounts of green tea for 30 minutes, at 12 V (a). (b) Different time of electrolysis from 15 to 45 minutes using 1 g of green tea at a constant voltage of 12 V. Inset pictures show the color change of the reaction solutions. Figure

S2: UV-vis spectrum of bio-AgNPs using grapefruit peel extracts synthesized at different masses of grapefruit peel (a), the applied DC voltage (b), and time of synthesis reaction (c), respectively. Inset pictures of glass vitals of reaction solutions. Figure S3: mechanism of forming silver nanoparticles from grapefruit peel extract. Figure S4: XRD spectrum of bio-AgNPs synthesized from grapefruit peel extract (a) and mangosteen peel extract (b). Figure S5: UV-vis spectrum of bio-AgNPs synthesized from three extracts of green tea (a), grapefruit peel (b), and mangosteen peel (c) in the presence of Fe (III) ions. Inset images show the color change of the solution after the addition of Fe (III) ions. Figure S6: UV-vis absorption spectroscopy and photo of bio-AgNP GTE in the presence of Fe (III) ions at a determined concentration at a concentration of 1 μM, 8 μM, and 14 μM measuring sensor with lake water sample. (The experiment was repeated 3 times with the same conditions). Figure S7: the linear relationship between the SPR band intensity and the concentration of Fe (III) ions using bio-AgNP GTE sensor measured with lake water sample (A_{425} and A_{440} is the absorbance of the ion bio-AgNP GTE in the absence and presence of corresponding Fe (III) ions, respectively). Figure S8: FTIR spectra of bio-AgNP GTE spectrum with Fe (III) ion addition. *(Supplementary Materials)*

References

[1] G. Cao, *Nanostructures and Nanomaterials*, Published by Imperial College Press and Distributed by World Scientific Publishing Co., 2004.

[2] V. V. Mody, R. Siwale, A. Singh, and H. R. Mody, "Introduction to metallic nanoparticles," *Journal of Pharmacy & Bioallied Sciences*, vol. 2, no. 4, pp. 282–289, 2010.

[3] I. Díez and R. H. A. Ras, "Fluorescent silver nanoclusters," *Nanoscale*, vol. 3, no. 5, pp. 1963–1970, 2011.

[4] V. Ahluwalia, S. Elumalai, V. Kumar, S. Kumar, and R. S. Sangwan, "Nano silver particle synthesis using *Swertia paniculata* herbal extract and its antimicrobial activity," *Microbial Pathogenesis*, vol. 114, pp. 402–408, 2018.

[5] X. Yan, B. He, L. Liu et al., "Antibacterial mechanism of silver nanoparticles in Pseudomonas aeruginosa: proteomics approach," *Metallomics*, vol. 10, no. 4, pp. 557–564, 2018.

[6] M. Konop, T. Damps, A. Misicka, and L. Rudnicka, "Certain aspects of silver and silver nanoparticles in wound care: a minireview," *Journal of Nanomaterials*, vol. 2016, Article ID 7614753, 10 pages, 2016.

[7] A. U. Khan, M. Khan, and M. M. Khan, "Antifungal and antibacterial assay by silver nanoparticles synthesized from aqueous leaf extract of Trigonella foenum-graecum," *Bionanoscience*, vol. 9, no. 3, pp. 597–602, 2019.

[8] S. Galdiero, A. Falanga, M. Vitiello, M. Cantisani, V. Marra, and M. Galdiero, "Silver nanoparticles as potential antiviral agents," *Molecules*, vol. 16, no. 10, pp. 8894–8918, 2011.

[9] Z. Bedlovičová, I. Strapáč, M. Baláž, and A. Salayová, "A brief overview on antioxidant activity determination of silver nanoparticles," *Molecules*, vol. 25, no. 14, p. 3191, 2020.

[10] C. Balagna, S. Perero, E. Percivalle, E. V. Nepita, and M. Ferraris, "Virucidal effect against coronavirus SARS-CoV-2 of a silver nanocluster/silica composite sputtered coating," *Open Ceramics*, vol. 1, p. 100006, 2020.

[11] Z. A. Ratan, M. F. Haidere, M. Nurunnabi et al., "Green chemistry synthesis of silver nanoparticles and their potential anticancer effects," *Cancers*, vol. 12, no. 4, p. 855, 2020.

[12] P. Yin, H. Li, C. Ke et al., "Intranasal Delivery of Immunotherapeutic Nanoformulations for Treatment of Glioma Through in situ Activation of Immune Response [Corrigendum]," *International Journal of Nanomedicine*, vol. Volume 15, pp. 8873-8874, 2020.

[13] K. B. Narayanan and N. Sakthivel, "Green synthesis of biogenic metal nanoparticles by terrestrial and aquatic phototrophic and heterotrophic eukaryotes and biocompatible agents," *Advances in Colloid and Interface Science*, vol. 169, no. 2, pp. 59–79, 2011.

[14] M. Rai, K. Kon, A. Ingle, N. Duran, S. Galdiero, and M. Galdiero, "Broad-spectrum bioactivities of silver nanoparticles: the emerging trends and future prospects," vol. 98, no. 5, pp. 1951–1961, 2014.

[15] S. Ahmed, M. Ahmad, B. L. Swami, and S. Ikram, "A review on plants extract mediated synthesis of silver nanoparticles for antimicrobial applications: a green expertise," *Journal of Advanced Research*, vol. 7, no. 1, pp. 17–28, 2016.

[16] X. Zhang, Z. Liu, W. Shen, and S. Gurunathan, "Silver nanoparticles: synthesis, characterization, properties, applications, and therapeutic approaches," vol. 17, no. 9, p. 1534, 2016.

[17] X.-Y. Dong, Z.-W. Gao, K.-F. Yang, W.-Q. Zhang, and L.-W. Xu, "Nanosilver as a new generation of silver catalysts in organic transformations for efficient synthesis of fine chemicals," *Catalysis Science & Technology*, vol. 5, no. 5, pp. 2554–2574, 2015.

[18] A. Loiseau, V. Asila, G. Boitel-Aullen, M. Lam, M. Salmain, and S. Boujday, "Silver-based plasmonic nanoparticles for and their use in biosensing," *Biosensors*, vol. 9, no. 2, p. 78, 2019.

[19] M. Yusuf, "Silver nanoparticles: synthesis and applications," in *Handbook of Ecomaterials*, pp. 2343–2356, Springer Nature, 2019.

[20] M. N. Nadagouda, T. F. Speth, and R. S. Varma, "Microwave-assisted green synthesis of silver nanostructures," *Accounts of Chemical Research*, vol. 44, no. 7, pp. 469–478, 2011.

[21] J. Pulit, M. Banach, and Z. Kowalski, "Chemical Reduction as the Main Method for Obtaining Nanosilver," *Journal of Computational and Theoretical Nanoscience*, vol. 10, no. 2, pp. 276–284, 2013.

[22] K. Ranoszek-Soliwoda, E. Tomaszewska, E. Socha et al., "The role of tannic acid and sodium citrate in the synthesis of silver nanoparticles," *Journal of Nanoparticle Research*, vol. 19, no. 8, p. 273, 2017.

[23] S. M. Landage, "Synthesis of nanosilver using chemical reduction methods," *International Journal of Advanced Research in Engineering and Applied Sciences*, vol. 3, no. 5, pp. 14–22, 2014.

[24] M. Xing, L. Ge, M. Wang, Q. Li, X. Li, and J. Ouyang, "Nanosilver particles in medical applications: synthesis, performance, and toxicity," *International journal of nanomedicine*, vol. 9, pp. 2399–2407, 2014.

[25] A. B. Seabra and N. Durán, "Nanotoxicology of metal oxide nanoparticles," *International Journal of Nanomedicine*, vol. 5, no. 2, pp. 934–975, 2015.

[26] S. Prabhu and E. K. Poulose, "Silver nanoparticles: mechanism of antimicrobial action, synthesis, medical applications, and toxicity effects," *International Nano Letters*, vol. 2, no. 1, pp. 32–41, 2012.

[27] A. K. Mittal, Y. Chisti, and U. C. Banerjee, "Synthesis of metallic nanoparticles using plant extracts," *Biotechnology Advances*, vol. 31, no. 2, pp. 346–356, 2013.

[28] P. Rauwel, S. Küünal, S. Ferdov, and E. Rauwel, "A review on the green synthesis of silver nanoparticles and their morphologies studied via TEM," *Advances in Materials Science and Engineering*, vol. 2015, Article ID 682749, 9 pages, 2015.

[29] V. V. Makarov, A. J. Love, O. V. Sinitsyna, S. S. Makarova, and I. V. Yaminsky, "Green' nanotechnologies: synthesis of metal nanoparticles using plants," vol. 6, no. 20, pp. 35–44, 2014.

[30] P. Singh, Y. Kim, D. Zhang, and D. Yang, "Biological synthesis of nanoparticles from plants and microorganisms," *Trends in Biotechnology*, vol. 34, no. 7, pp. 588–599, 2016.

[31] P. Agarwal, V. K. Bairwa, S. Kachhwaha, and S. L. Kothari, "Green synthesis of silver nanoparticles using callus extract of Capsicum annuum L. and their activity against microorganisms," *International Journal of Nanotechnology and Application*, vol. 4, no. 5, pp. 1–8, 2014.

[32] M. Rafique, I. Sadaf, M. S. Rafique, and M. B. Tahir, "A review on green synthesis of silver nanoparticles and their applications," *Artificial Cells, Nanomedicine, and Biotechnology*, vol. 45, no. 7, pp. 1272–1291, 2017.

[33] G. Gahlawat and A. R. Choudhury, "A review on the biosynthesis of metal and metal salt nanoparticles by microbes," *RSC Advances*, vol. 9, no. 23, pp. 12944–12967, 2019.

[34] P. C. Nagajyothi, S. E. Lee, M. An, and K. D. Lee, "Green synthesis of silver and gold nanoparticles using Lonicera Japonica flower extract," *Bulletin of the Korean Chemical Society*, vol. 33, no. 8, pp. 2609–2612, 2012.

[35] A. Ebrahiminezhad, A. Zare-Hoseinabadi, A. K. Sarmah, S. Taghizadeh, Y. Ghasemi, and A. Berenjian, "Plant-mediated synthesis and applications of iron nanoparticles," *Molecular Biotechnology*, vol. 60, no. 2, pp. 154–168, 2018.

[36] J. Y. Song and B. S. Kim, "Rapid biological synthesis of silver nanoparticles using plant leaf extracts," *Bioprocess and Biosystems Engineering*, vol. 32, no. 1, pp. 79–84, 2009.

[37] P. Tippayawat, N. Phromviyo, P. Boueroy, and A. Chompoosor, "Green synthesis of silver nanoparticles in aloe vera plant extract prepared by a hydrothermal method and their synergistic antibacterial activity," *PeerJ*, vol. 4, p. e2589, 2016.

[38] R. Geethalakshmi and D. V. L. Sarada, "Characterization and antimicrobial activity of gold and silver nanoparticles synthesized using saponin isolated from *Trianthema decandra* L.," *Industrial Crops and Products*, vol. 51, pp. 107–115, 2013.

[39] M. Sökmen, S. Y. Alomar, C. Albay, and G. Serdar, "Microwave assisted production of silver nanoparticles using green tea extracts," *Journal of Alloys and Compounds*, vol. 725, pp. 190–198, 2017.

[40] S. Hussain and Z. Khan, "Epigallocatechin-3-gallate-capped Ag nanoparticles: preparation and characterization," *Bioprocess and Biosystems Engineering*, vol. 37, no. 7, pp. 1221–1231, 2014.

[41] Q. Sun, X. Cai, J. Li, M. Zheng, Z. Chen, and C. P. Yu, "Green synthesis of silver nanoparticles using tea leaf extract and evaluation of their stability and antibacterial activity," *Colloids and Surfaces A: Physicochemical and Engineering Aspects*, vol. 444, pp. 226–231, 2014.

[42] W. R. Rolim, M. T. Pelegrino, B. de Araújo Lima et al., "Green tea extract mediated biogenic synthesis of silver nanoparticles: Characterization, cytotoxicity evaluation and antibacterial activity," *Applied Surface Science*, vol. 463, pp. 66–74, 2019.

[43] D. Zhan, X. Li, A. B. Nepomnyashchii, M. A. Alpuche-Aviles, F. R. F. Fan, and A. J. Bard, "Characterization of Ag^+ toxicity on living fibroblast cells by the ferrocenemethanol and oxygen response with the scanning electrochemical microscope," *Journal of Electroanalytical Chemistry*, vol. 688, pp. 61–68, 2013.

[44] J. Xu, Y. Zhou, S. Liu, M. Dong, and C. Huang, "Low-cost synthesis of carbon nanodots from natural products used as a fluorescent probe for the detection of ferrum(iii) ions in lake water," *Analytical Methods*, vol. 6, no. 7, pp. 2086–2090, 2014.

[45] V. Kumar, S. Mohan, D. K. Singh, D. K. Verma, V. K. Singh, and S. H. Hasan, "Photo-mediated optimized synthesis of silver nanoparticles for the selective detection of Iron(III), antibacterial and antioxidant activity," *Materials Science and Engineering: C*, vol. 71, pp. 1004–1019, 2017.

[46] K. Lertsuwan, K. Nammultriputtar, S. Nanthawuttiphan et al., "Differential effects of Fe2+ and Fe3+ on osteoblasts and the effects of 1,25(OH)2D3, deferiprone and extracellular calcium on osteoblast viability under iron-overloaded conditions," *PLoS One*, vol. 15, no. 5, pp. e0234009–e0234023, 2020.

[47] V. K. Gupta, N. Mergu, and L. K. Kumawat, "A new multifunctional rhodamine-derived probe for colorimetric sensing of Cu(II) and Al(III) and fluorometric sensing of Fe(III) in aqueous media," *Sensors and Actuators B: Chemical*, vol. 223, pp. 101–113, 2016.

[48] C. R. Lohani and K. H. Lee, "The effect of absorbance of Fe^{3+} on the detection of Fe^{3+} by fluorescent chemical sensors," *Sensors and Actuators B: Chemical*, vol. 143, no. 2, pp. 649–654, 2010.

[49] A. Kamal, N. Kumar, V. Bhalla, M. Kumar, and R. K. Mahajan, "Rhodamine-dimethyliminocinnamyl based electrochemical sensors for selective detection of iron (II)," *Sensors and Actuators B: Chemical*, vol. 190, pp. 127–133, 2014.

[50] X. Chen, Q. Zhao, W. Zou, Q. Qu, and F. Wang, "A colorimetric Fe3+ sensor based on an anionic poly(3,4-propylenedioxythiophene) derivativeA colorimetric Fe3+ sensor based on an anionic poly(3,4-propylenedioxythiophene) derivative," *Sensors and Actuators B: Chemical*, vol. 244, pp. 891–896, 2017.

[51] X. Xing, Y. Yang, T. Zou et al., "Thioglycolic acid-capped ZnSe quantum dots as nanoprobe for cobalt(II) and iron(III) via measurement of grey level, UV-vis spectra and dynamic light scattering," *Microchimica Acta*, vol. 186, no. 7, pp. 26–31, 2019.

[52] C. Chen, X. Zhang, P. Gao, M. Hu, and M. Hu, "A water stable europium coordination polymer as fluorescent sensor for detecting Fe^{3+}, CrO_4^{2-}, and $Cr_2O_7^{2-}$ ions," *Journal of Solid State Chemistry*, vol. 258, pp. 86–92, 2018.

[53] K. S. Rao, T. Balaji, T. P. Rao, Y. Babu, and G. R. K. Naidu, "Determination of iron, cobalt, nickel, manganese, zinc, copper, cadmium and lead in human hair by inductively coupled plasma-atomic emission spectrometry," *Spectrochimica Acta Part B: Atomic Spectroscopy*, vol. 57, no. 8, pp. 1333–1338, 2002.

[54] M. Soylak and A. Aydin, "Determination of some heavy metals in food and environmental samples by flame atomic absorption spectrometry after coprecipitation," *Food and Chemical Toxicology*, vol. 49, no. 6, pp. 1242–1248, 2011.

[55] S. P. Wu, Y. P. Chen, and Y. M. Sung, "Colorimetric detection of Fe3+ ions using pyrophosphate functionalized gold nanoparticles," *Analyst*, vol. 136, no. 9, pp. 1887–1891, 2011.

[56] X. Gao, Y. Lu, S. He, X. Li, and W. Chen, "Colorimetric detection of iron ions (III) based on the highly sensitive plasmonic response of the *N*-acetyl-l-cysteine-stabilized silver nanoparticles," *Analytica Chimica Acta*, vol. 879, pp. 118–125, 2015.

[57] B. Singh, J. P. Singh, A. Kaur, and N. Singh, "Phenolic composition, antioxidant potential and health benefits of citrus peel," *Food Research International*, vol. 132, article 109114, 2020.

[58] K. N. Mahmud and Z. A. Zakaria, "Pyrolytic products from oil palm biomass and its potential applications," in *Valorisation of Agro-industrial Residues–Volume II: Non-Biological Approaches*, pp. 225–236, Springer, Cham, 2020.

[59] A. S. Zarena and K. Udaya Sankar, "Xanthones enriched extracts from mangosteen pericarp obtained by supercritical carbon dioxide process," *Separation and Purification Technology*, vol. 80, no. 1, pp. 172–178, 2011.

[60] K. S. Siddiqi, A. Husen, and R. A. K. Rao, "A review on biosynthesis of silver nanoparticles and their biocidal properties," *Journal of nanobiotechnology*, vol. 16, no. 1, p. 14, 2018.

[61] G. Serdar, E. Demir, S. Bayrak, and M. Sökmen, "New approaches for effective microwave assisted extraction of caffeine and catechins from green tea," *International Journal of Secondary Metabolite*, vol. 3, no. 1, pp. 3–13, 2016.

[62] R. D. Rivera-Rangel, M. P. González-Muñoz, M. Avila-Rodriguez, T. A. Razo-Lazcano, and C. Solans, "Green synthesis of silver nanoparticles in oil-in-water microemulsion and nanoemulsion using geranium leaf aqueous extract as a reducing agent," *Colloids and Surfaces A: Physicochemical and Engineering Aspects*, vol. 536, pp. 60–67, 2018.

[63] B. Banumathi, B. Vaseeharan, P. Suganya et al., "Toxicity of Camellia sinensis-Fabricated Silver Nanoparticles on Invertebrate and Vertebrate Organisms: Morphological Abnormalities and DNA Damages," *Journal of Cluster Science*, vol. 28, no. 4, pp. 2027–2040, 2017.

[64] D. Kumar, G. Kumar, and V. Agrawal, "Green synthesis of silver nanoparticles using Holarrhena antidysenterica (L.) Wall. bark extract and their larvicidal activity against dengue and filariasis vectors," *Parasitology Research*, vol. 117, no. 2, pp. 377–389, 2018.

[65] S. S. K. Kamal, P. K. Sahoo, J. Vimala, M. Premkumar, S. Ram, and L. Durai, "A novel green chemical route for synthesis of silver nanoparticles using Camellia sinensis," *Acta Chimica Slovenica*, vol. 57, no. 4, pp. 808–812, 2010.

[66] L. O. Cinteza, C. Scomoroscenco, S. Voicu et al., "Chitosan-stabilized ag nanoparticles with superior biocompatibility and their synergistic antibacterial effect in mixtures with essential oils," *Nanomaterials*, vol. 8, no. 10, p. 826, 2018.

[67] S. Thatai, P. Khurana, S. Prasad, and D. Kumar, "A new way in nanosensors: gold nanorods for sensing of Fe(III) ions in aqueous media," *Microchemical Journal*, vol. 113, pp. 77–82, 2014.

[68] Y. L. Zhang, L. Wang, H. C. Zhang et al., "Graphitic carbon quantum dots as a fluorescent sensing platform for highly efficient detection of Fe3+ ions," *RSC Advances*, vol. 3, no. 11, pp. 3733–3738, 2013.

[69] A. Ananthanarayanan, X. Wang, P. Routh et al., "Facile synthesis of graphene quantum dots from 3D graphene and their application for Fe3+ sensing," *Advanced Functional Materials*, vol. 24, no. 20, pp. 3021–3026, 2014.

[70] J. Ju and W. Chen, "Synthesis of highly fluorescent nitrogen-doped graphene quantum dots for sensitive, label-free detection of Fe (III) in aqueous media," *Biosensors & Bioelectronics*, vol. 58, pp. 219–225, 2014.

[71] S. Bian, C. Shen, H. Hua et al., "One-pot synthesis of sulfur-doped graphene quantum dots as a novel fluorescent probe for highly selective and sensitive detection of lead(II)," *RSC Advances*, vol. 6, no. 74, pp. 69977–69983, 2016.

[72] C. Guo and J. Irudayaraj, "Fluorescent Ag clusters via a protein-directed approach as a Hg(II) ion sensor," *Analytical Chemistry*, vol. 83, no. 8, pp. 2883–2889, 2011.

[73] X. Yuan, T. J. Yeow, Q. Zhang, J. Y. Lee, and J. Xie, "Highly luminescent Ag+ nanoclusters for Hg2+ ion detection," *Nanoscale*, vol. 4, no. 6, pp. 1968–1971, 2012.

[74] M. Annadhasan, T. Muthukumarasamyvel, V. R. Sankar Babu, and N. Rajendiran, "Green synthesized silver and gold nanoparticles for colorimetric detection of Hg 2+, Pb 2+, and Mn 2+ in aqueous medium," *ACS Sustainable Chemistry & Engineering*, vol. 2, no. 4, pp. 887–896, 2014.